Volume 61
Number 97
18 December 2025
Pages 19135–19322

ChemComm

Chemical Communications

rsc.li/chemcomm

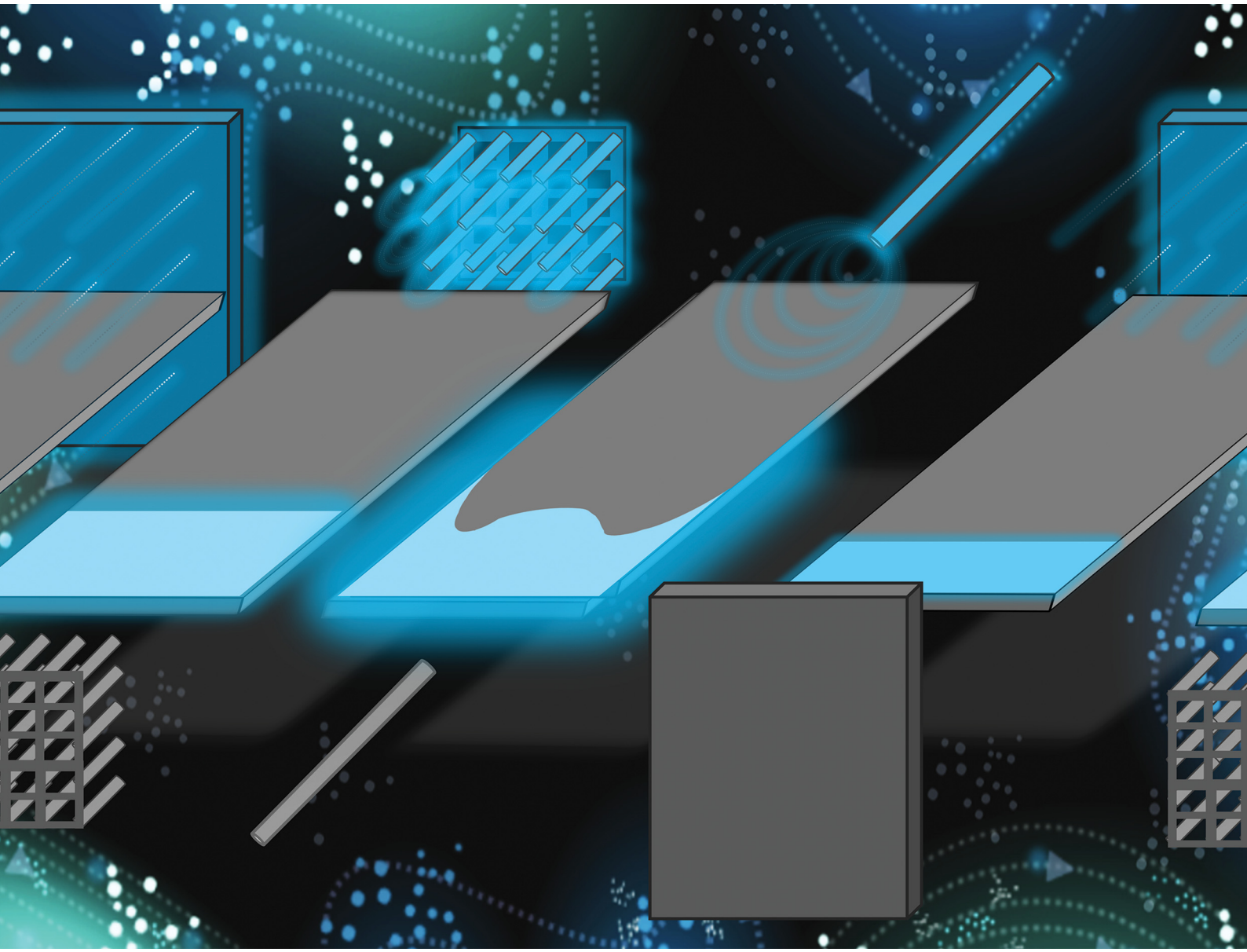

ISSN 1359-7345

ROYAL SOCIETY OF CHEMISTRY

COMMUNICATION

Robert J. Forster *et al.*

Directing the glow: 3D feeder geometries to enhance planar bipolar electrochemiluminescence

ChemComm

COMMUNICATION

View Article Online
View Journal | View Issue

Cite this: *Chem. Commun.*, 2025, **61**, 19221

Received 15th August 2025,
Accepted 21st October 2025

DOI: 10.1039/d5cc04706d

rsc.li/chemcomm

Directing the glow: 3D feeder geometries to enhance planar bipolar electrochemiluminescence

Oisín Foley Doyle, [a] Gordon G. Wallace, [c] Zhilian Yue, [c] Jun Chen, [c] Stephen Beirne [c] and Robert J. Forster *[ab]

Using 3D-printed pin arrays or single wires as feeders in open bipolar cells enhances luminol bipolar electrochemiluminescence (BP-ECL) and allows light to be generated in localised regions of planar stainless-steel bipolar electrodes (BPEs). Spatially resolved ECL mapping shows that both pin arrays and single wires outperform planar feeders, yielding approx. 2-fold and 2.6-fold more intense ECL, respectively. Strikingly, single-wire feeders produce a symmetrical three-spot emission pattern, while planar and pin array feeders generate uniform bands of ECL. These findings demonstrate that compact feeder architectures can localise and intensify BP-ECL, enabling efficient wire-free electrochemical activation without the need for size matching of the feeder and the BPE.

Controlling the spatial distribution of the induced potential and the current flow within bipolar electrochemical cells is key to developing next-generation wireless electrochemical technologies, including multianalyte sensors, adaptive (4D) materials, microreactors, and electrocatalytic platforms.[1,2] The local potential difference that drives redox reactions at a bipolar electrode, BPE, does not exclusively arise from a static electric field in a uniform dielectric medium, but from an electric potential gradient controlled by ionic current flow through the electrolyte. This gradient reflects the combined effects of the applied voltage between feeder electrodes, the solution conductivity, and the faradaic or capacitive processes at both the feeders and the BPE surface. Thus, the potential induced in the BPE depends critically on the dynamic current flow, rather than simple geometric field lines generated by the potential difference between the feeders.

In planar configurations, where two extended feeder electrodes are positioned on either side of a planar BPE, the potential difference across the electrolyte develops gradually along the cell axis (x-direction) and can be tuned by adjusting the spacing of the feeders as well as the applied voltage.[3] When the widths of the feeders and the BPE are comparable, the potential variation across the electrode width (y-direction) is approximately uniform. Under these conditions, the potential difference within the BPE reflects the local distribution of solution potential along its length, which in turn depends on the spatial pattern of ionic current flow between the feeders. By deliberately shaping the feeder electrodes or varying their separation, the current paths, and therefore the solution potential, can be tailored to achieve controlled, spatially selective polarisation within the BPE.

Three-dimensional feeder electrodes, such as 3D-printed Ti_6Al_4V pin arrays, allow the potential and current distribution within the electrolyte to be controlled. Local curvature, field focusing, and fringing effects around the protruding pins on each feeder array can introduce anisotropic potential gradients that modulate the direction and magnitude of ionic fluxes.[4] In turn, they control the induced voltage not only along the traditional x-axis, but also in the transverse y-direction. By controlling these gradients, it becomes possible to tune where and at what rate redox reactions occur across the BPE surface, potentially enabling spatially resolved electrocatalysis, reagent generation, or sensing zones on a single, continuous electrode.

To visualise and quantify how variations in feeder geometry and current pathways shape the local potential and reaction zones on a BPE surface, several wireless mapping techniques have been developed. Wireless electropolymerisation of conducting monomers such as EDOT or pyrrole has been used as a qualitative indicator of local potential distribution.[5] Polymer deposition occurs close to those regions where the interfacial potential exceeds the oxidative threshold, thereby identifying regions of high anodic polarisation. However, the spatial resolution of this method is limited by the fact that polymer may not necessarily deposit exactly where radicals are electrogenerated, due to diffusion, ionic migration, and convection, effects that are especially pronounced in complex 3D geometries where the potential distribution is strongly non-uniform.

Bipolar electrochemiluminescence (BP-ECL) offers a complementary, non-destructive approach with superior spatial and

[a] *School of Chemical Sciences, Dublin City University, Dublin 9, Ireland. E-mail: robert.forster@dcu.ie*
[b] *FutureNeuro, SFI Research Centre for Chronic and Rare Neurological Diseases, Dublin City University, Dublin 9, Ireland*
[c] *Intelligent Polymer Research Institute, Faculty of Engineering and Information Science, University of Wollongong, Innovation Campus, North Wollongong, NSW, 2500, Australia*

temporal resolution.[6–8] Because light emission occurs only when the local interfacial potential surpasses the activation threshold for ECL generation, BP-ECL can allow zones of electrochemical activity to be visualised in real time without altering the electrode surface. When combined with image-based analysis, the spatial intensity profiles provide a more quantitative insight into the underlying potential and current distributions and can help discriminate whether the rate-determining step is mass transport or heterogeneous electron transfer.

Here, a custom-designed electrochemical cell was created *via* CAD and 3D-printed using tough PLA filament. The internal cell volume was approximately 3.0 cm^3. The cell contains 3 cm^3 of 10 mM Luminol and 30 mM H_2O_2 in 0.1 M NaOH solution. The nominal electric field strength was kept constant at 3.33 V cm^{-1}, typically 10 V dropped across 3 cm ignoring ohmic losses. Differences in the ECL generating regions and ECL intensity can be used to elucidate how different feeder geometries affect the potential in solution and hence within the BPE. Here, the ECL intensity along five separate line plots from the BPE terminal (0 cm) towards the centre of the BPE (1 cm) were used to map the local ECL intensity.

When a planar BPE is placed between two planar, perpendicular feeders, the solution potential varies progressively across the electrode in accordance with the imposed current flow.[9] Fig. 1 shows a typical experimental ECL intensity profile across a planar electrode where the feeders are two vertical, planar electrodes. Several key observations can be made. First, no light is observed for distances greater than approximately 0.12 cm from the tip of the bipolar anode. Cyclic voltammetry experiments using a traditional 3-electrode cell and a highly sensitive PMT for ECL detection indicate that a potential of 0.33 V is required to generate luminol ECL under these conditions.

The BPE is 2.0 cm long and the voltage at its centre is at 0 V while at 0.872 cm (1–0.128 cm, the first location light is observed), it is 0.33 V. Thus, while the nominal field strength is 3.33 V cm^{-1}, the actual field strength is approximately 0.38 V cm^{-1}. In part, the significantly reduced field reflects iR drop between the feeder and bipolar electrodes. Second, the variation in ECL intensity with *x*-distance is not linear for any *y*-position on the bipolar electrode. Non-linearity is expected if the rate of heterogeneous electron transfer, *k*, is rate limiting since *k* depends exponentially on the overpotential. It is also important to consider the possibility that mass transport may limit the ECL response closer to the anode tip where the overpotential, and consequently the rate of heterogeneous electron transfer, are largest. However, the potential at the tip of the bipolar electrode is expected to be approximately 0.38 V, *i.e.*, 0.38 V cm^{-1} × 1.0 cm, giving a maximum overpotential driving heterogeneous electron transfer of only about 50 mV. The luminol ECL reaction involves bond breaking and formation, and it is highly likely that the reorganisation energy is of the order of 0.5–1.0 eV.[10] Therefore, slow heterogeneous electron transfer rather than mass transfer by diffusion/migration is the most likely rate determining step, RDS, across the entire BPE where ECL is generated, *i.e.*, a change of RDS in ECL generation does not contribute to the non-linear dependence of I_{ECL} on distance.

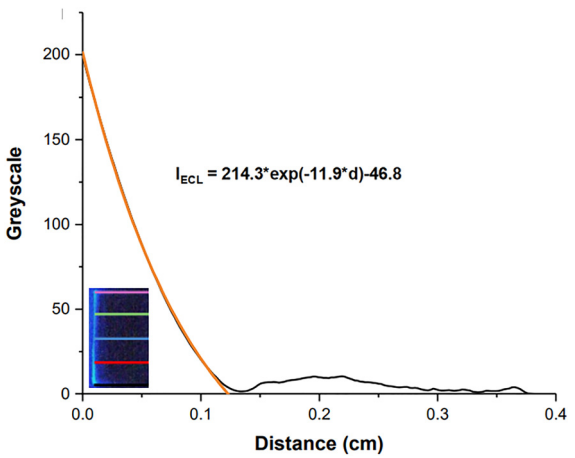

Fig. 1 An averaged ECL intensity (greyscale) *vs.* distance plot across the 2 cm long (*x*) by 1 cm wide (*y*) centred, planar BPE. The inset shows a top-down view of the ECL generated at the BPE and the location of the experimentally indistinguishable, individual traces that were averaged to obtain the black line of the main figure.

Marcus theory predicts an exponential dependence of the current density or rate of heterogeneous electron transfer on the overpotential, η, (= $E_{app} - E^{\circ\prime}$, where E_{app} is the applied potential and $E^{\circ\prime}$ is the operational formal potential) at least when the overpotential is small.[11] Fig. 1 shows that a very high-quality fit (R^2 = 0.9995) is obtained for the experimental I_{ECL} *vs.* distance (voltage) profile for the bipolar cell with a planar BPE and planar feeders using I_{ECL} = 214.3 ± 72.1 × exp(−11.9 ± 1.2 × *d*) −46.8 ± 20.0, where *d* is the distance measured from the tip of the BPE anode, *i.e.*, where the overpotential is largest. The high-quality fit further suggests that the ECL profile is controlled by heterogeneous electron transfer kinetics, influenced by the voltage induced across the bipolar electrode.

The electrochemiluminescence (ECL) intensity along a bipolar electrode decreases exponentially with distance from the anode tip because even if the local interfacial potential difference decreases linearly under a uniform electric field the redox reaction rate governing ECL depends exponentially on the (over)potential. Significantly, the best fit equation can be used to accurately determine the distance from the tip over which ECL is generated. This value, 0.128 cm, agrees with that found by measuring the distance from the ECL image using Image J, but has the significant advantage of using the bright ECL response, (S/N ratio is > 20) to accurately determine the distance rather than trying to identify the first "bright" pixel where the S/N ratio can be less than 1. The observation that the best fit requires a negative offset, −46.8 ± 20.0 a.u., likely arises because the standard heterogeneous electron transfer rate, k°, is not zero, but other effects, such as limited detector sensitivity (8-bit), ambient light, non-uniform electric fields, reagent depletion/transport or excited state quenching, may also be important. Numerical integration gives an overall ECL intensity, ϕ, of 16.1 ± 3.6 for the planar feeder systems which can provide a convenient way to compare alternative systems using different feeder electrode types.

Three-dimensional feeder structures, such as a single pin electrode oriented in the same plane as the BPE, could give a highly localised, intense potential distributions since it should

act as a point-like electric field source, creating a strongly radial electric field that dissipates sharply in a lateral (y) direction. The ability to localise ECL could significantly impact sensor development. For example, the detection region could be switched when the analytical performance degrades locally or different analytes could be detected at different physical locations on the BPE, *i.e.*, spatially resolved multianalyte detection, but where the detector performance can be optimised for each analyte without having a bright adjacent emission due to another analyte.

Significantly, as shown in Fig. 2, a single wire feeder creates a focused polarisation region in the BPE directly facing the wire feeder tip, but two additional bright ECL regions are observed at the lateral edges of the BPE. Line scans of the ECL intensity *vs.* x-distance at different y-locations can provide a deeper insight into the electric field distribution and how feeder electrode configuration can be used to spatially manipulate ECL active regions on the BPE.

Fig. 2 demonstrates that there are significant differences in the ECL intensity line scans between the centre of the BPE that is directly opposite the single wire feeder, 2.5 mm away from the centre and the edges. For example, like the full-width planar feeder, the intensity of the line scans at the middle of the BPE, and the two either side (2.5 mm away) decrease exponentially from the edge of the BPE facing the wire feeder. Fitting all three of these traces close to the centres of the BPE indicates that the width of the ECL generating region is 0.198 ± 0.02 cm, corresponding to a field of 0.41 ± 0.01 V cm^{-1}, which is approximately 10% higher than that found for the planar feeders. In contrast, while significant ECL is observed at the edges of the BPE where there is no opposing feeder, I_{ECL} is initially high, but is independent of the x-distance for the first 0.11 cm before decaying exponentially with increasing distance. Significantly, ECL is observed for substantially longer distances at the edges, 0.30 and 0.39 cm for the right and left edges, respectively, corresponding to fields of 0.46 ± 0.05 and 0.54 ± 0.06 V cm^{-1}. It

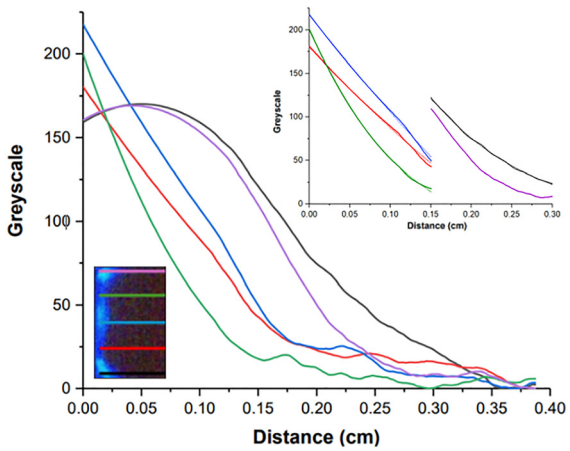

Fig. 2 ECL intensity (greyscale) *vs.* distance plots (n = 3) at five different positions across the surface of a 2 cm long by 1 cm wide planar BPE where the feeder electrodes are single titanium wires (0.1 cm dia) located in the same plane as the BPE and centred. The inset shows a top-down view of the ECL generated at the BPE and the locations of the ECL profiles are colour coded to the graphs.

may be important to note that the asymmetry may arise due to the single wire feeder not being placed in the exact centre of the BPE.

These are the highest field strengths observed and exceed the planar feeder values by 20 to 40%. While the predicted overpotential is relatively larger, *e.g.*, 0.21 V at the left edge, this is unlikely to be sufficient to observe a Marcus inverted region effect even if mass transport limitations (due to diffusion and migration in the field) were absent. The observation of isolated ECL at the corners of the BPE, even though there is no physical feeder opposite arises because the electric fields at the lateral edges of the feeder wire (left and right edges), fringe outwards. This fringing increases the normal component of the electric field at those edge locations, leading to localised enhancements in the current flow and potential drop across the BPE–solution interface. These effects are amplified by the sharp corner and the small thickness of the BPE, 0.1 cm. Fringing is especially prominent in this configuration due to the highly non-uniform electric field distribution caused by the miniaturised (0.1 cm diameter cylinder) feeder. The central placement and symmetry of the single wire feeder promotes a mirror-symmetric potential distribution across the BPE, encouraging approximate equivalent activation of both terminal regions. Finally, the path of least resistance for ionic current flow from the feeder to the BPE is not strictly linear and the current paths can curve laterally through the electrolyte, resulting in spatially diffuse field lines that can reach terminal regions with sufficient strength to drive bipolar reactions. Significantly, using a single wire feeder results in the highest integrated ECL intensity, ϕ, among all feeder configurations investigated at 41.6 ± 4.9 AU. The higher total emission intensity observed arises in large part due to a larger emitting region because of the potential distribution. Thus, using a single 3D pin feeder can give heterogeneous potential distributions in solution, allowing the polarisation to be spatially confined at the BPE and enabling lower feeder voltages to be used for a given ECL system.

To probe the effect of using multiple pins as feeders, an array was used as the feeder electrode where the long axis of the pins is in the same plane as the bipolar electrode. The array comprises twenty-five round cylinders (0.015 cm radius, 0.3 cm long) that are evenly separated on a 0.48 cm × 0.48 cm square-porous base (total geometric area of 1.32 cm^2). Importantly, the array is 0.48 cm wide compared to the 1 cm width of the BPE, and it is centrally located in both y and z. The pins are expected to act as point sources of electric field and the electric field lines could diverge radially from the pins and converge toward the BPE. However, fringing at the edges could extend the ECL generating region into areas where the feeder is not present as observed for the single wire system. The change in feeder material from pure titanium to Ti_6Al_4V is reasonable because both materials exhibit similar electrochemical stability and oxide-forming behaviour in aqueous media. The small alloying additions of aluminium and vanadium do not significantly alter the surface potential or conductivity under the conditions used, so the overall behaviour of the bipolar electrode remains largely unchanged.

Fig. 3 illustrates five ECL intensity line scans obtained for the planar BPE surface but where pin arrays are used as feeders. The ECL intensities measured at the anodic edge are clustered

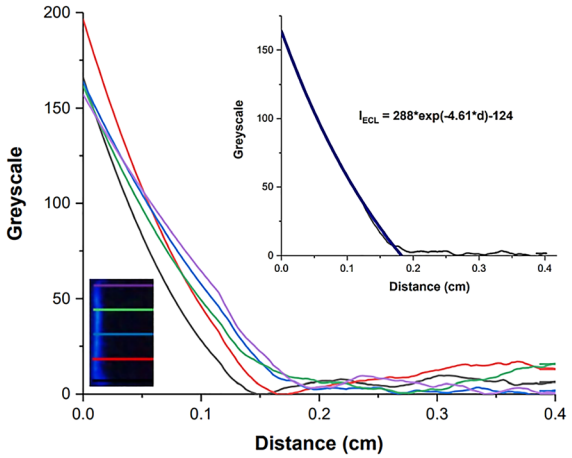

Fig. 3 ECL intensity (greyscale) *vs.* distance plots (n = 3) at five distinct positions across the surface of a 2 cm long by 1 cm wide planar BPE where the feeder electrodes are 3D-printed Ti_4Al_6V pin arrays located in the same plane as the BPE and centred. The small lower inset to the left shows a top-down view of the ECL generated at the BPE and the locations of the ECL profiles are colour coded to the graphs. Inset to right shows the average of the five experimental traces and the best fit single exponential decay.

tightly within a narrow range, 178 ± 13 and cannot be experimentally distinguished. This close grouping indicates that the potential distribution in solution and hence across the BPE is highly uniform (y-direction) and that fringing very significantly extends the width of the ECL generating region, *i.e.*, the feeder array is only 0.48 cm wide, but uniform ECL is generated across the entire 1.0 cm width of the BPE. The striking uniformity of the ECL arises because the lateral arrangement of the pins causes the electric fields from neighbouring pins to converge when moving away from the pin array surface and, at the relatively remote (5 mm from the feeder) bipolar electrode the potential distribution is homogeneous. This superposition effect gives rise to broader and more spatially uniform ECL. Significantly, while the actual electric field strength obtained experimentally using the planar and pin array feeders, 0.380 and 0.395 V cm^{-1}, respectively, and the maximum ECL intensities at the anode tips are indistinguishable, the integrated ECL intensity, ϕ, is approximately double (32.0 ± 2.5 *vs.* 16.1 ± 3.6) when the feeder is a pin array. This larger total light emission using a pin array as feeders arises due to a larger ECL emission region, 0.125 to 0.175 cm, *i.e.*, a 40% increase in emitting area. However, it is important to consider the role of iR drop between the feeder and bipolar electrodes. While the area of each individual pin is relatively small, radial spreading significantly increases the volume through which current can effectively flow through solution. Each pin's radial current path addresses a large volume of electrolyte, effectively lowering the total solution resistance relative to the planar feeder electrodes of equivalent projected geometric area. This reduced iR drop changes the ECL intensity *vs.* distance profiles with the pin array feeder showing making the spatial decay rate lower and giving a brighter emission.

This work demonstrates that changing the geometry of the feeder electrode is a powerful approach to controlling the location and intensity of BP-ECL. Planar feeders, which have the same width as the bipolar electrode induce the same potential across the full width of the BPE which is ideal for applications requiring consistent light output across large areas, *e.g.*, ultrasensitive detection since the total light intensity is high because of the large area. In striking contrast, a single wire feeder produces a focused ECL hotspot directly opposite its tip, with secondary emissions at the BPE edges due to localised current flow and fringing electric fields giving a spatial pattern that can be exploited to localise analytical responses. The location and relative intensity of the three emitting areas can be controlled by changing the size and position of the feeder relative to the BPE, as well as the width and thickness of the BPE itself. Pin arrays, despite being narrower than the BPE, generate ECL across the entire BPE width by distributing the electric field radially, activating more of the BPE through 3D field spreading.

Miniaturised 3D feeders and BPEs can harness lightning-rod field amplification to overcome the higher potentials normally required when miniaturised bipolar electrodes are used. In conclusion, feeder design emerges as a powerful lever for creating low-power, addressable and wire-free means of redefining what is possible in bipolar electrochemical sensing, bioassays, and light-generating devices.

The financial support of Research Ireland (SFI) under Grant Number 21/FFP-P/10255 and the EU under MSCA Doctoral Network ECLectic (101119951) is gratefully acknowledged. This publication has emanated from research supported in part by a research grant from Research Ireland (SFI) under 21/RC/10294_P2 and co-funded under the European Regional Development Fund and by FutureNeuro industry partners. The authors wish to acknowledge the use of facilities at the Australian National Fabrication Facility (ANFF) – Materials Node at the University of Wollongong.

Conflicts of interest

There are no conflicts to declare.

Data availability

The data supporting the findings of this study are available within the article.

References

1 Y.-L. Wang, *et al.*, *ChemistryOpen*, 2022, **11**(12), e202200163.
2 O. F. Doyle and R. J. Förster, *Electrochem. Commun.*, 2024, **169**, 107832.
3 M. Wagner, *et al.*, *ChemElectroChem*, 2025, **12**(6), e202400506.
4 Y. Koizumi, *et al.*, *Nat. Commun.*, 2016, **7**(1), 10404.
5 Á. Brady, *et al.*, *Chem. Commun.*, 2024, **60**(89), 13000–13003.
6 R. Zou, *et al.*, *Chem. Commun.*, 2025, **61**, 11896–11906.
7 E. Villani, *Electrochemistry*, 2024, **92**(10), 101007.
8 L. Bouffier and N. Sojic, Introduction and overview of electrogenerated chemiluminescence, in *Analytical Electrogenerated Chemiluminescence*, ed. N. Sojic, Royal Society of Chemistry, Cambridge, 2019, pp. 1–28.
9 R. M. Crooks, Principles of Bipolar Electrochemistry, *ChemElectroChem*, 2016, **3**(3), 357–359.
10 C. Mariani, *et al.*, *Electrochim. Acta*, 2024, **489**(10), 144256.
11 J. Wang, *et al.*, *Nat. Commun.*, 2021, **12**(1), 6333.

